

Theory of optically induced molecular reorientations and quantitative experiments on wave mixing and the self-focusing of light

I. C. Khoo

Department of Physics and Astronomy, Wayne State University, Detroit, Michigan 48202

(Received 18 September 1981)

We present a theoretical treatment of optical-field-induced molecular reorientations and quantitative experimental verifications of the associated nonlinear-optical processes in the nematic phase of liquid crystals. Explicit analytic expressions are obtained in the small-angle linearized approximation of the Euler-Lagrange equation describing the molecular reorientation. It is found that optical-field strengths much lower than the so-called optical Freedericksz transition threshold can create substantial molecular reorientations and generate easily observable nonlinear-optical effects such as self-focusing and degenerate four-wave mixings. The theoretically predicted dependences on the scattering geometry, the optical intensities, and the nematic thicknesses are in excellent agreement with experimental data. The relative contribution of thermal effect is also determined.

I. INTRODUCTION

The physics of liquid crystals is a complex but fascinating subject. In particular, their optical properties have been the subject of intensive fundamental and applied investigation.¹ Recently, the nonlinear-optical properties of nematic liquid crystals under the action of purely optical and dc-plus-optical fields have received considerable attention.²⁻⁹

In brief, the action of an optical field on nematics is in many respects equivalent to a dc field. Specifically, the interaction can be described by the addition of a term $(8\pi)^{-1}\Delta\epsilon E_{\text{op}}^2$ in the free energy (where $\Delta\epsilon$ is the optical dielectric anisotropy and E_{op}^2 the optical-field strength). Because the nematic's response times are generally very long, only the time independent (i.e., dc) component in E_{op}^2 will manifest. In that sense, the process of optically inducing molecular reorientation is almost identical to the now well-known dc-field-induced distortion of nematics.¹ On the other hand, because optical fields involve propagation and the inevitable nonuniformity in the intensity (field) distribution of the light beam, there are several questions that deserve a detailed analysis. Explicit analytical descriptions of the various effects associated with geometry, polarization, thicknesses, etc., are missing from the literature, even though they may be somehow deduced from our understanding of the nematic's dc-field responses.

In this paper, we present an approximate solution of the Euler-Lagrange equation that allows an identification of the optical nonlinearities and easy and direct comparison with experiments. The accuracy of the approximation is negligible, in fact, compared to many other more frequently made assumptions, (e.g., the one-constant approximation) in some of the so-called exact solution.¹⁰ Detailed comparison of the theoretical expressions with the experiments on wave mixing and the self-focusing of lights shows that within the limits defining the validity of our approximations, excellent agreements are obtained. In addition, other mechanisms that also contribute to these nonlinear-optical processes, e.g., thermal indexing, can be quantitatively determined. This paper is a natural and necessary extension of the preliminary study as reported in Ref. 4, and will answer some of the questions that may be raised on the rather new subject of optical-field-induced nonlinearity in nematics.

II. THEORY

We will divide our theoretical discussion into subsection A the molecular reorientation, subsection B the optical nonlinearity, and subsection C the thermal effect.

A. Molecular reorientation

Without much loss of generality, consider a homeotropically aligned nematic liquid-crystal film

with an incident optical field. (To treat a planar structure, one merely needs to substitute in the appropriate elastic constant.) The geometry is depicted in Fig. 1. The unperturbed director axis $\hat{n}(0)$ is along Z . The optical propagation is in the XZ plane, with the optical propagation vector \hat{k} making an angle β with the Z axis. In the presence of an optical field, therefore, the angle between \hat{k} and $\hat{n}(I)$ is given by $\psi = \beta + \theta$. A solution of the Maxwell's equations for the anisotropic medium in this configuration immediately yields, for the effective dielectric constant ϵ_{eff} ,

$$\epsilon_{\text{eff}} = \frac{\epsilon_{\perp} \epsilon_{\parallel}}{\epsilon_{\parallel} \cos^2 \psi + \epsilon_{\perp} \sin^2 \psi}, \quad (1)$$

where ϵ_{\parallel} and ϵ_{\perp} have their usual meaning. The reorientation angle θ is obtained by minimizing the free energy of the system:

$$F = \frac{K}{2} \{ [\vec{\nabla} \cdot \hat{n}(\vec{r})]^2 + [\vec{\nabla} \times \hat{n}(\vec{r})]^2 \} - \frac{\Delta \epsilon}{8\pi} [\vec{E}_{\text{op}} \cdot \hat{n}(\vec{r})]^2, \quad (2)$$

where K is the elastic constant (i.e., we have made a one-constant approximation). This procedure yields the well-known Euler-Lagrange equation (a sine-Gordon equation) describing the so called "torque" balance between the reorientating "force" from the optical field and the elastic restoring force.

$$\xi^2 \frac{\partial^2 \theta}{\partial Z^2} + \sin \psi \cos \psi = 0, \quad (3)$$

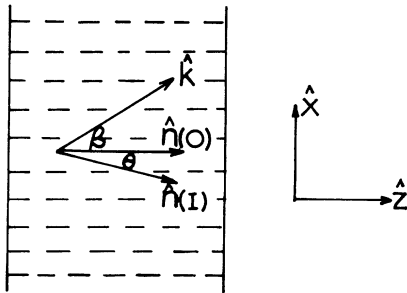


FIG. 1. Relative orientation between the director axis and the optical propagation in a homeotropically aligned sample.

where

$$\xi^2 = 4\pi K (\Delta \epsilon)^{-1} E_{\text{op}}^{-2}.$$

We have assumed, of course, an infinite plane wave, which is accurate for typical nematic film thicknesses and laser beam sizes.

The solution of Eq. (3) is a well-known elliptic integral¹⁰ from which it is not immediately obvious how the intensity-dependent dielectric constant may be extracted. To be specific, if one desires to evaluate an intensity-dependent dielectric constant in the form

$$\epsilon_{\text{eff}} = \epsilon_0 + \delta \epsilon(I), \quad (4)$$

where $\delta \epsilon(I)$ is linear in the intensity I (for the purpose of studying third order nonlinear-optical processes, for example) these analytical solutions are not very useful.

A small-angle approximate solution of Eq. (3) however, appears to serve this particular purpose, namely, the identification of $\delta \epsilon(I)$ very well. It is also very accurate as we will demonstrate in a later section. Assuming hard boundary conditions, i.e., $\theta = 0$ at $Z = 0$ and at $Z = d$, where d is the film thickness, Eq. (3) can be rewritten as

$$2\xi^2 \frac{d^2 \theta}{dZ^2} + (2 \cos 2\beta) \theta + \sin 2\beta = 0. \quad (5)$$

Define

$$\phi = (2 \cos 2\beta) \theta + \sin 2\beta. \quad (6)$$

Equation (5) can be rewritten as

$$\left[\frac{\xi^2}{\cos 2\beta} \right] \frac{d^2 \phi}{dZ^2} + \phi = 0. \quad (7)$$

The solution of ϕ , subject to the conditions $\theta = 0$ at $Z = 0$ and at $Z = d$, is

$$\phi = \sin 2\beta \left[\cos \left[\frac{Z}{\xi'} \right] + \frac{\left[1 - \cos \frac{d}{\xi'} \right]}{\sin \left[\frac{d}{\xi'} \right]} \sin \frac{Z}{\xi'} \right], \quad (8)$$

where $\xi' = (\xi^2 / \cos 2\beta)^{1/2}$.

For a weak optical field, i.e., where $d^2 / \xi^2 \ll 1$ [or equivalently, $E_{\text{op}}^2 \ll E_{\text{th}}^2$, where E_{th} , the optical

Frederickz threshold,⁴ is given by $E_{th}^2 = 4\pi^3 K(\Delta\epsilon)^{-1} d^{-2}$], one can easily show that $Z/\xi < d/\xi \ll 1$. Equations (6) and (8) give upon expansion of the sine and cosine term inside the square bracket of (8)

$$\theta \sim \frac{1}{2} \sin 2\beta \left[\frac{dZ}{2\xi^2} - \frac{Z^2}{2\xi^2} \right]. \quad (9)$$

Note that θ is maximum ($\theta = \theta_{max}$) at $Z = d/2$, which is expected from symmetry consideration

$$\theta_{max} = \frac{\sin 2\beta}{16\xi^2 d^{-2}}.$$

An immediate conclusion one can draw is that optical-field strengths well below the so-called Fredericksz threshold can induce substantial molecular reorientations. For instance, if $\sin 2\beta = 0.5$, and $16\xi^2 d^{-2} = 25$ [i.e., $E_{op}^2 = 0.2E_{th}^2$], then Eq. (9) gives $\theta_m \sim 0.02$. In a later section, we find that this corresponds to a change (linear in θ) in refractive index of 0.005. For a typical MBBA film of $75 \mu\text{m}$ thick the optical threshold field (in terms of the intensity) is estimated to be about 100 W/cm^2 . (Please see last paragraph of this section.) Hence one requires only an optical intensity on the order of 20 W/cm^2 to induce such a large non-linearity. On the other hand, to achieve a comparable change in a well-known nonlinear liquid like CS_2 , for example, would have required intensity on the order of GW/cm^2 .¹¹

B. The optical nonlinearity

As a result of the reorientation of the molecules, the effective dielectric constant as given by Eq. (2), after some rearrangement of terms become

$$\epsilon_{eff} \approx \epsilon_{\perp} \left[1 + \frac{\Delta\epsilon}{\epsilon_{\parallel}} \sin^2(\beta + \theta) \right] \quad (10)$$

$$\sim \epsilon_{\perp} \left[1 + \frac{\Delta\epsilon}{\epsilon_{\parallel}} (\beta^2 + \theta^2 + 2\beta\theta) \right] \quad (11)$$

$$\sim \epsilon_{\perp} + \delta\epsilon(\beta) + \delta\epsilon(\theta) + \delta\epsilon(\theta^2). \quad (12)$$

The first two terms on the rhs of Eq. (12) are the unperturbed components, corresponding to the effective dielectric constant as seen by an optical field propagating such that \hat{k} makes an angle β with the Z axis, along which the unperturbed director axis points. The third term is the contribution from the molecular reorientation. Note that $\delta\epsilon(\theta)$ is proportional to E_{op}^2 , i.e., it is the intensity-dependent dielectric constant. The last term is proportional to E_{op}^4 (or I^2) and is not of our interest here. It is interesting to note here that the magnitude of these terms are comparable to each other. Nevertheless, we will limit our discussion to the intensity-dependent term $\delta\epsilon(\theta)$. From (9) and (11), we have

$$\delta\epsilon = \frac{\Delta\epsilon \epsilon_{\perp} \beta \sin 2\beta}{2\epsilon_{\parallel} \xi^2} (dZ - Z^2);$$

note:

$$\xi^{-2} \sim E_{op}^2. \quad (13)$$

So far we have assumed that there is only one incident field of wave vector \vec{k} . It is straightforward to generalize the above results to the case of several optical fields with different propagation vectors, assuming again that all the frequencies are the same. It is perhaps important to point out here that nematics' responses are slow. Typically, the response time τ (which may be roughly taken as the sum of the turn on and the turn off times) is on the order of deciseconds to seconds, depending on several factors. If there is a frequency offset ($\Delta\omega$, say) between the incident fields, then the scattering cross section is reduced³ by a factor of $(1 + \Delta\omega\tau)$. In practical terms, this would mean that the incident laser fields have to be of the same frequency to reorient the molecules.

If there are two fields of propagation constant \vec{k}_1 and \vec{k}_2 , then E_{op}^2 become

$$E_1 E_1^* + E_2 E_2^* + E_1 E_2^* \exp(i(\vec{k}_1 - \vec{k}_2) \cdot \vec{r}) + E_2 E_1^* \exp(i(\vec{k}_2 - \vec{k}_1) \cdot \vec{r}).$$

The last two terms contribute to spatially varying dielectric constants (i.e., grating), and give rise to degenerate four-wave mixings. Diffractions occur along \vec{k}_4 determined by $\vec{k}_4 = 2\vec{k}_1 - \vec{k}_2$ and $\vec{k}_4 = 2\vec{k}_2 - \vec{k}_1$, respectively, as is well known.

For one incident optical field, the intensity-dependent dielectric constant given in (13) gives rise to nonlinear self-phase modulation of the beam as it propagates through the nematic film. For most laser beams with a intensity profile (e.g., a

Gaussian), self-focusing⁵ will result, since $\delta\epsilon$ as obtained in Eq. (13) is positive.

It is perhaps outside the scope of this paper to present a rigorous treatment of the theory of self-focusing. Reference can be made, of course, to some rather comprehensive treatment.¹² For the purpose of quantitative comparison with theory, we note that if the incident laser has a Gaussian distribution of beam waist r_0 , and the nonlinearity is of the form $\epsilon_{\text{eff}} = \epsilon_0 + \delta\epsilon(I)$ then the self-focusing distance f is given in the thin lens limit to be

$$f^{-1} \simeq dr_0^{-2} \delta\epsilon(I) \simeq \frac{I \Delta\epsilon^2 \epsilon_1 d^3 r_0^{-2} \beta \sin 2\beta}{2C\epsilon_{\parallel} K}, \quad (14)$$

where we have used the integrated (over the thickness d) value of $\delta\epsilon(\theta)$, and express the result in terms of the optical intensity $I = (C/8\pi)E_{\text{op}}^2$. It is important to note here that the focusing power f^{-1} scale as d^3 and is proportional to the geometrical factor $\beta \sin\beta \cos\beta$.

C. The thermal effect

The analysis of nematics' response would have been much simpler if orientational mechanism alone had been responsible for the nonlinearity. In nematic liquid crystal, another mechanism, namely, thermal indexing ($d\epsilon/dT$) also account for the two nonlinear-optical processes as mentioned above. In this case, the intensity-dependent dielectric constant is due to absorption of the laser and subsequent thermalization.

For a quantitative determination of the contribution from thermal effect, we recall that for nematics, $d\epsilon_{\parallel}/dT$ is negative and $d\epsilon_{\perp}/dT$ is positive where T denotes the temperature. From Eq. (1), the change in the effective dielectric constant associated with a rise in temperature of dT is given by (assuming $\Delta\epsilon/\epsilon_{\parallel}$ is $\ll 1$)

$$\frac{d\epsilon_{\text{eff}}}{dT} \approx \frac{d\epsilon_{\perp}}{dT} \cos^2\beta + \frac{d\epsilon_{\parallel}}{dT} \sin^2\beta. \quad (15)$$

Writing

$$\frac{d\epsilon_{\parallel}}{dT} = -\gamma \frac{d\epsilon_{\perp}}{dT},$$

we get

$$\frac{d\epsilon_{\text{eff}}}{dT} = \frac{d\epsilon_{\perp}}{dT} [1 - (\gamma + 1) \sin^2\beta]. \quad (16)$$

We have also approximated $\beta + \theta$ by β since β is much greater than θ . For most nematics, $\gamma > 1$ throughout the nematic (temperature) range.¹³ For MBBA at room temperature, for example, $\gamma \approx 5$. The change in dielectric constant associated with a temperature rise dT is therefore given by

$$\delta\epsilon(dT) = d\epsilon_{\perp}(dT) [1 - (\gamma + 1) \sin^2\beta]. \quad (17)$$

We note that $d\epsilon_{\perp}(dT)$ is linear in the optical intensity and we write it as $\alpha_{\text{th}}I$. Combining Eqs. (17) and (13), the total dielectric constant change associated with molecular reorientation and thermal effect is given by

$$\delta\epsilon_{\text{total}} = \delta\epsilon(\theta) + \delta\epsilon(dT). \quad (18)$$

When β is small, for all intents and purposes, $\sin^2\beta = \beta \sin\beta \cos\beta$. Hence one can write

$$\delta\epsilon_{\text{total}} = I [\alpha_{\theta} - \alpha_{\text{th}}(\gamma + 1)] \times \beta \sin\beta \cos\beta + I \alpha_{\text{th}}, \quad (19)$$

where α_{θ} denotes the contribution from orientational mechanism and may be deduced from Eq. (13). α_{th} denotes the thermal contribution. Roughly, $\alpha_{\text{th}} \propto d$. If integrated over the sample thickness d , α_{θ} gives $\bar{\alpha}_{\theta}$ and α_{th} gives $\bar{\alpha}_{\text{th}}$. Note that $\bar{\alpha}_{\theta}$ is proportional to d^3 while $\bar{\alpha}_{\text{th}}$ is proportional to d^2 . Referring to (14), we observe therefore that if thermal effects are included, then f^{-1} is nonvanishing for $\beta = 0$, i.e., at normal incidence, self-focusing will occur due to thermal lensing effect. Thermal lensing effect was observed by Volterra and Wiener-Avnear⁷ in 1974, who were then not aware of the possibility of optical-field-induced molecular reorientational effect.

For easy reference, we note here that for MBBA, typical values for the various molecular constants appearing in (19) are $K \approx 0.8 \times 10^{-6}$ dynes; $\Delta\epsilon = 0.4$, $\gamma \approx 5$ at room temperature (20°C). Also, defining a threshold intensity $I_{\text{th}} = (CE_{\text{th}}^2/8\pi)10^{-7}$ (in W/cm^2), we note that for a 100- μm thick MBBA sample, $I_{\text{th}} \approx 100 \text{W}/\text{cm}^2$. I_{th} scales as d^{-2} so that a 50- μm thick sample would have an optical Freedericksz threshold intensity of 400 W/cm^2 .

III. EXPERIMENTS

Our experiments are aimed at testing the dependences on the geometry (i.e., on β) and on the thickness as predicted in the preceding equations, and also the numerical value of f^{-1} and the wave-mixing efficiency. Experimental results on degenerate four-wave mixings have been reported

before. We mention here two important points that have not been treated, namely, the dependence on the angle β and the thermal contribution. The insert in Fig. 2 shows the scattering geometry. The 5145-Å line of a Argon laser is divided into two roughly equal intensity beams and then combined (with a small crossing angle) on the sample with their propagation vector \hat{k}_1 and \hat{k}_2 making an angle β with the molecule's director axis direction (Z). The sample is a homeotropically aligned MBBA film of 75 μm thick at room temperature (20°C). One of the nonlinearly diffracted beam (which lies in the plane defined by \hat{k}_1 and \hat{k}_2) is monitored.

Figure 2 shows the diffracted intensity plotted as a function of $(\beta \sin\beta \cos\beta)^2$. It can be shown that the diffraction is proportional to $(\delta\bar{\epsilon})^2$ where $\delta\bar{\epsilon}$ is the integrated value of $\delta\epsilon$ (over the thickness d). The plot shows a straight line passing through the origin, in excellent agreement with the theoretical prediction. From Eq. (17), we note that thermal effect would have caused a nonzero contribution. The results therefore confirmed that thermal grating is not significant at low optical intensity. It is important to remind ourselves here that we are using optical field well below the Freedericksz threshold. The intensity used in this experiment is

about 5 W/cm², for I_1 and 3 W/cm² for I_2 , whereas the Freedericksz threshold corresponds to an intensity on the order of 180 W/cm².

The large nonlinearity associated with optically induced molecular reorientation is reflected by the readiness with which the beams self-focus. At $\beta \approx 25^\circ$, denoted SF in Fig. 2, all exit beams clearly show that they have self-focused. It is interesting to note here the rather low intensity, namely, 3 to 5 W/cm² that is required to produce self-focusing effect.

Perhaps the most immediate question about wave mixing is what happens at normal incidence if the incident optical intensity is increased. In fact, it was observed that at $\beta=0$, a nonzero wave-mixing efficiency (i.e., a clearly visible diffraction) is observed if the incident optical intensity is increased to about 20 W/cm² ($I_1 \approx 20$ W/cm², $I_2 \approx 12$ W/cm²). We suspect that this could be due to the small but nevertheless finite thermal grating effect. To perform a quantitative check of this, we note that the diffraction in the $2\hat{k}_1 - \hat{k}_2$ direction, following well-known wave-mixing calculation, is given by

$$I_D \sim (I^{-1} \delta\bar{\epsilon}_{\text{tot}}) I_1^2 I_2 \\ \sim (I^{-1} \delta\bar{\epsilon}_{\text{tot}}) I_L^3,$$

where I_L is the intensity of the incident laser (before it is split into I_1 and I_2). For a fixed I_D , $I_L^{-3/2}$ is therefore given by

$$I_L^{-3/2} \sim [\bar{\alpha}_\theta - \bar{\alpha}_{\text{th}}(\gamma + 1)] \beta \sin\beta \cos\beta + \bar{\alpha}_{\text{th}}. \quad (20)$$

Experimentally, we increase the incident intensity till a diffraction is observed and its intensity I_D recorded. The experiment is then repeated for various value of β .

Figure 3 is a plot of $I_L^{-3/2}$ versus the geometrical factor $\beta \sin\beta \cos\beta$. A linear dependence, in accordance with the theory, is clearly obtained with a nonzero intercept at $\beta=0$. It is interesting to note that the intensity required to generate the same magnitude of diffraction drops from 20 W/cm² (for $\beta=0$) to only 4 W/cm² (for $\beta=25^\circ$).

From Eq. (20), the intercept at $\beta=0$ is clearly proportional to $\bar{\alpha}_{\text{th}}$, while the slope is proportional to $\bar{\alpha}_\theta - \bar{\alpha}_{\text{th}}(\gamma + 1)$. The ratio of these two quantities; i.e., slope/(intercept) is therefore

$$-(\gamma + 1) + \frac{\bar{\alpha}_\theta}{\bar{\alpha}_{\text{th}}} \approx -6 + \frac{\bar{\alpha}_\theta}{\bar{\alpha}_{\text{th}}}$$

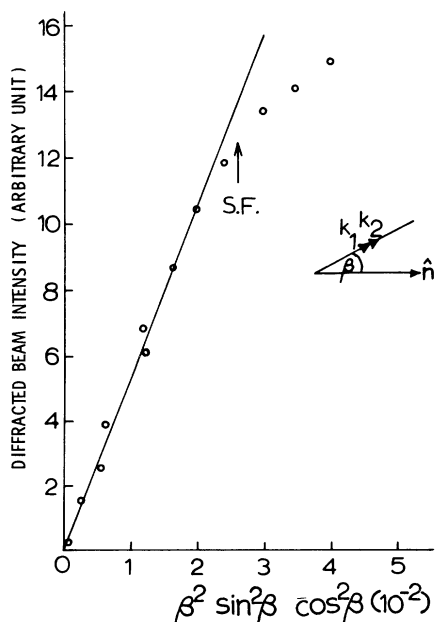


FIG. 2. The dependence of the diffracted intensity on the geometrical factor. Insert shows a schematic of the scattering geometry.

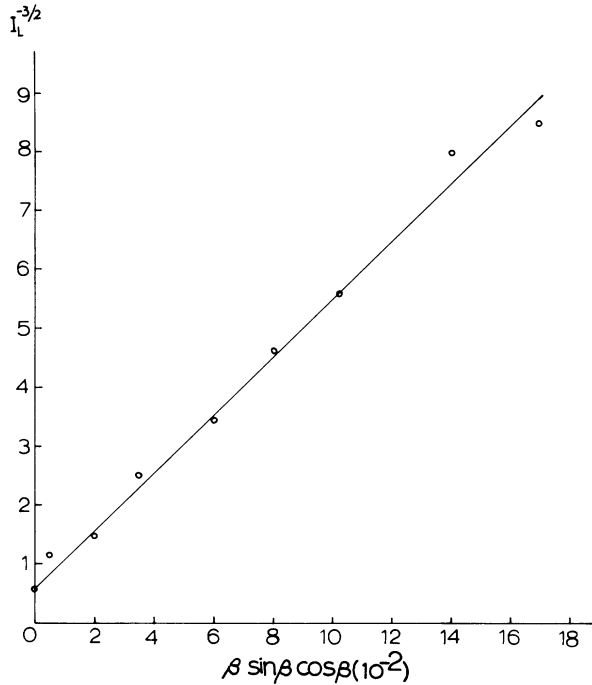


FIG. 3. The diffraction at higher optical intensity showing thermal effect.

for MBBA at room temperature (when $\gamma=5$). From Fig. 3, slope is 53 and the intercept is 0.5. This gives $\bar{\alpha}_\theta/\bar{\alpha}_{th} \approx 112$. In other words, the orientational contribution is much greater than the thermal grating effect. Since the magnitude of the orientational nonlinearity is determined also by the factor $\beta \sin \beta \cos \beta (\approx \beta^2)$, we note that the orientational and the thermal contributions will be comparable for $\beta \lesssim 0.1$ (when $\bar{\alpha}_\theta \beta^2 \approx \bar{\alpha}_{th}$, $\beta \approx 0.1$). For larger angle, the orientational contribution will therefore dominate.

It is perhaps superfluous but important to remind ourselves here that thermal contribution only matter at high optical intensity ($I_1 \gtrsim 20$ W/cm²). For $I_1 \approx 5$ W/cm², as in the case mentioned earlier with reference to Fig. 2, there is practically no observable wave mixing at $\beta=0$.

It is also appropriate at this juncture to clarify some of the points made in Ref. 4. From our study of the wave mixing in a tilted geometry, and the fact that optical field well below the Fredericksz transition can induce molecular reorientation (and therefore wave mixing), we now know that the diffractions observed in Ref. 4 is most likely due to the optical reorientation in a tilted geome-

try. In Ref. 4, the incident laser was not strictly at normal incidence (i.e., $\beta \neq 0$). A review of the experimental situation shows that the laser was incident at about 10° (i.e., $\beta = 10^\circ$) in order to avoid reflection feedback to the laser. Our present study shows that indeed the geometrical dependence is a rather drastic one: at $I_1 = 5$ W/cm² and $I_2 = 3$ W/cm², the diffraction increases from zero to a clearly visible beam as β is increased from 0° to 10°.

Our study at *higher* optical intensities ($I_1 = 20$ W/cm²) has further established that at small β (i.e., near normal incidence), *both* orientational and thermal mechanisms contribute (for MBBA, of course). If strictly orientationally related diffractions were of interest, one condition will be to set $\beta \geq 0.3$, which, for a 75- μ m thick sample, gives a relative thermal contribution of less than 10%.

Finally, if we examine the numerical value of the conversion efficiently, we found that there is a very good agreement between the theory and experiment. Following the usual wave-mixing calculation as exemplified in Refs. 3 and 4, and assuming a more correct value of $\Delta\epsilon = 0.4$ (not 0.1 as used in Ref. 4), we get

$$I_D \approx 0.2 I_1^2 I_2 \beta^2 \sin^2 \beta \cos^2 \beta,$$

where we have ignored the thermal contribution by using only low-intensity optical beams. For $I_1 = 5$ W/cm² and $I_2 = 3$ W/cm², and $\beta = 0.17$ (i.e., 10°), we have experimentally obtained a conversion efficiency I_D/I_2 of 5×10^{-3} . The theoretically predicted value is 4×10^{-3} . This excellent agreement is probably very fortuitous, in view of several uncertainties. However, it clearly demonstrates the importance of accounting for the geometrical factor which in the above calculation gives a factor of 0.0004.

The self-focusing of light

The experimental setup is depicted in Fig. 4(a). An argon laser operating in the TEM₀₀ mode 5145 Å line is lightly focused by a converging lens with a focal length of 40 cm. The sample is placed at 45 cm from the lens. The estimated focus spot size (r_0) at the sample is 2×10^{-3} cm². Homeotropic MBBA films of 25, 50, and 75 μ m thick are used. The far field intensity distribution is projected on a board 8 m away.

Self-focusing of the laser as it propagates through the sample is manifested in the form of a

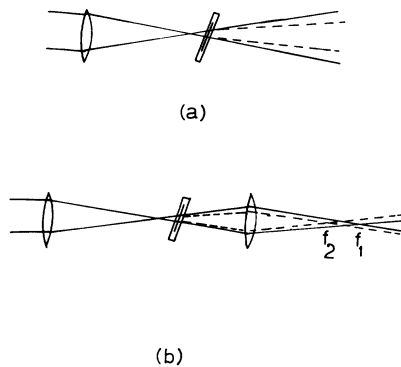


FIG. 4. (a) Schematics of the experimental setup for observing self-focusing. (b) Schematics for showing the positive power of the nematic film.

decrease in the divergence of the beam. It has been observed⁶ that as the intensity of the laser is increased, rings begin to appear, a phenomenon that was also observed in Ref. 7. These rings were due to the phase modulation experienced by the laser because of the intensity-dependent refractive index. Its number seems to correspond to the theoretical prediction $N = (\text{phase shift})/2\pi$ very well.

When these rings appear, quantitative studies of the self-focusing of light become very complicated. We have instead concentrated our studies on the intensification of the central region as a result of the self-focusing. By putting a small aperture on the exit beam central region and measuring the normalized intensity $In (I_{\text{transmitted}}/I_{\text{incident}})$, we have in fact noticed a more than 4 times increase in In when the beam self-focused. The central bright spot has a fairly well-defined divergence that changes as the intensity is raised and can be quantitatively measured.

Before we proceed to discuss our experimental results, we have further established the self-focusing property of the nematic film using the simple geometrical setup as shown in Fig. 4(b). The two converging lens form a focus at f_1 in the absence of the the nematic film. When the film is inserted, and when the laser intensity is raised, the focus of the optical system is clearly shifted to f_2 , which can only happen if the nematic has a positive power.

We have made two quantitative measurements, one dealing with the case where thermal lensing effect is absent, and the other involving contribution from the thermal effect.

In the first experiment, we use a low-intensity beam and study the divergence of the beam as the

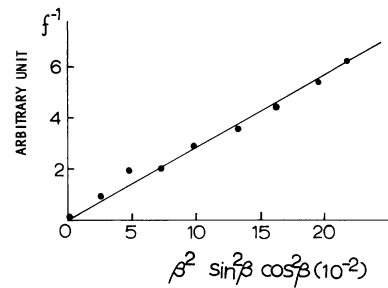


FIG. 5. The dependence of the focusing power on the geometrical factor.

sample is tilted (i.e., vary β). The intensity is adjusted so that self-focusing is not observed at normal incidence but shows up as β is increased; we have also made sure that the intensity is not strong enough to generate diffraction rings.

Figure 5 shows a plot of the power f^{-1} of the nematic as a function of the geometrical factor, for an incident optical intensity of 20 W/cm² on a 50- μm thick sample. A very good linear fit is obtained, in agreement with the theoretical prediction of Eq. (14). The numerical agreement between the experimental data and the theory is also very good. At $\beta=0.4$ (25°), the estimated value for f^{-1} from Eq. (14) based on the constants given in the last paragraph of the previous section is $\frac{1}{75} \text{ cm}^{-1}$ for an optical intensity of 20 W/cm². The experimental value for f^{-1} is $\frac{1}{20} \text{ cm}^{-1}$. These measured values of f^{-1} correspond to a change in dielectric constant (between the center of the beam and the e^{-2} intensity point) of 0.003. The agreement is fairly good, in view of the various approximations assumed in the theory and the uncertainties in the values of the molecular constant assumed. Nevertheless, the agreement between the theory and the experiment on the geometry dependence is particularly notable.

In the second experiment, the incident optical intensity ($I_{1/2}$) is varied to produce the same self-focused divergence in the exit beam. We choose the divergence to be half of the unperturbed beam. For a fixed divergence, and therefore f^{-1} , a plot of $I_{1/2}^{-1}$ versus the geometrical factor should be a straight line, following Eqs. (19) and (14). As the angle β is increased from 0 (i.e., tilted away from normal incidence), one would expect that $I_{1/2}$ to increase. From Eq. (19), one can see that the ratio of the slope to the intercept at $\beta=0$ should give $-(\gamma+1) + \bar{\alpha}_\theta/\bar{\alpha}_{\text{th}}$.

Figures 6(a) and (b) show a plot of $I_{1/2}^{-1}$ versus β for two samples of 25 and 50 μm thicknesses,

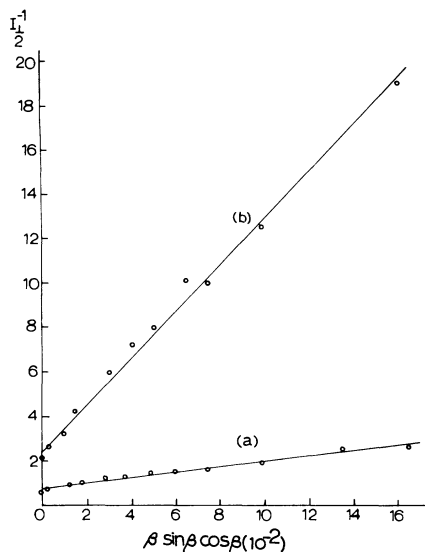


FIG. 6. Self-focusing at higher optical intensity: (a) for a 25- μm thick sample and (b) for a 50- μm thick sample.

respectively. In both cases, there is a finite intercept on the $I_{1/2}^{-1}$ axis (an artifact of our experiment, of course). The slope (for 50- μm sample) is found to be [106] unit, in comparison with the intercept of [2] units. The ratio is therefore 53. For room temperature (20°C) MBBA, $\gamma \approx 5$, and we have therefore $\bar{\alpha}_\theta/\bar{\alpha}_{\text{th}} = 59$. The magnitude of the reorientational nonlinear coefficient $\bar{\alpha}_\theta$, of course, depends on several factors such as $\Delta\epsilon$, K , both of which do not vary greatly for different nematics. However, $\bar{\alpha}_\theta$ depends crucially on the thickness d ($\bar{\alpha}_\theta \propto d^3$). On the other hand, the thermal coefficient is linear in d^2 . Therefore, the ratio of $\bar{\alpha}_\theta/\bar{\alpha}_{\text{th}}$ (for different thicknesses) should scale as d . Figure 6(b), which pertains to a thinner (25- μm thick) sample, shows precisely this point. The slope is measured to be 15 and the intercept is 0.6. The ratio is therefore 25. This therefore gives $(\bar{\alpha}_\theta/\bar{\alpha}_{\text{th}}) = 31$. Comparing this with the value of $(\bar{\alpha}_\theta/\bar{\alpha}_{\text{th}})$ obtained above for a 50- μm thick sample, we can see that the scaling as d of these ratios is indeed obeyed. The experimental data for a 75- μm thick sample is also consistent with this scaling. It is interesting to recall that the experiment on wave mixing as discussed earlier for a 75- μm sample gives $\bar{\alpha}_\theta/\bar{\alpha}_{\text{th}} = 112$, again supporting the thickness scaling dependence. Moreover, one can see from the intercepts in Fig. 6 that $\bar{\alpha}_{\text{th}}$ does vary roughly as d^2 .

The subject of the self-focusing of cw laser beams in nematics obviously can be pursued fur-

ther. However, we will content ourselves here with the rather remarkable agreement between the qualitative theory and the experimental results on the thickness and the geometry dependence, and the numerical value of the self-focusing distance.

IV. CONCLUSION

We have presented a quantitative theory and experimental treatment of optical-field-induced nonlinear effects in nematic liquid crystals. In the small-angle approximation, the agreement between theory and experiments are remarkable. Specifically, the measurement of the nonlinear processes (wave mixing and self-focusing) as a function of the geometrical factors have provided further quantitative understanding into nematics responses and thrown new lights on previous studies of degenerate wave-mixing process. Most importantly, we have shown that a weak optical field (well below the so-called Fredericksz transition) can create substantial molecular reorientation and therefore large nonlinear effects. The theoretical expressions obtained in our study, although approximate, are explicit and should provide a useful starting point for analyzing nematics' nonlinearities. Our method of obtaining the relative contribution of thermal effect should also be applicable to other nematics besides MBBA. Nevertheless, I should remark that the nonlinear interaction of nematics with light is a complicated issue; we have not, for example, studied the dynamics of the problem. One might also easily conjecture performing various counterpart studies of the now well-established dc-field-induced effects in nematics, since, as we remarked earlier, the action of an optical field is almost equivalent to a dc field. Because optical studies involve propagation, and also one has now the extra variable of adding on a dc field, it is expected that many interesting nonlinear electro-optical and magneto-optical effects will emerge.

ACKNOWLEDGMENTS

This research was supported by a grant from the National Science Foundation under Contract No. ECS 8026775. An equipment grant from the Research Corporation Cottrell Research Program is also acknowledged. The author is thankful to S. L. Zhuang, S. Shepard, and S. Nahar for their assistance. The interest and the encouragement of Professor Emmett Leith and some helpful conversations with Professor Y. R. Shen are also acknowledged.

- ¹See for example, E. B. Priestley, P. J. Wojtowicz, and P. Sheng, *Introduction to Liquid Crystal* (Plenum, New York, 1974); also, P. G. de Gennes, *The Physics of Liquid Crystal* (Clarendon, Oxford, 1974), and the numerous references therein.
- ²G. K. L. Wong and Y. R. Shen, *Phys. Rev. Lett.* **30**, 895 (1973); **32**, 527 (1974); J. W. Shelton and Y. R. Shen, *ibid.* **25**, 23 (1970); **26**, 538 (1971); S. K. Saha and G. K. L. Wong, *Opt. Commun.* **30**, 119 (1979). A comprehensive review may be seen in Y. R. Shen, *Rev. Mod. Phys.* **48**, 1 (1976).
- ³R. M. Herman and R. J. Serinko, *Phys. Rev. A* **19**, 1757 (1979).
- ⁴(a) I. C. Khoo, *Phys. Rev. A* **23**, 2077 (1981); (b) I. C. Khoo and S. L. Zhuang, *Appl. Phys. Lett.* **37**, 3 (1980).
- ⁵B. Ya Zel'dovich and N. V. Tabiryan, *Pis'ma Zh. Eksp. Teor. Fiz.* **30**, 510 (1979) [*JETP Lett.* **30**, 478 (1979)]; B. Ya Zel'dovich, N. F. Pilipetskii, A. V. Sukhov, and N. V. Tabiryan, *Pis'ma Zh. Eksp. Teor. Fiz.* **31**, 287 (1980) [*JETP Lett.* **31**, 263 (1980)].
- ⁶N. F. Pilipetski, A. V. Sukhov, N. V. Tabiryan and B. Ya Zel'dovich, *Opt. Commun.* **37**, 280 (1981); S. D. Durbin, S. M. Arakelian and Y. R. Shen, *Opt. Lett.* (in press).
- ⁷V. Volterra and E. Wiener-Aunear, *Opt. Commun.* **12**, 194 (1974).
- ⁸J. R. Lalanne, B. Martin, and B. Pouligny, *Mol. Cryst. Liq. Cryst.* **42**, 153 (1977); J. Prost and J. R. Lalanne, *Phys. Rev. A* **8**, 2090 (1973).
- ⁹I. C. Khoo, *Phys. Rev. A* **25**, 1040 (1982). This reference deals with nonlinear magneto-optical processes in nematics.
- ¹⁰See for example, S. I. Ben-Abraham, *Phys. Rev. A* **14**, 1251 (1976), and the references therein. See also P. Pincus, *J. Appl. Phys.* **41**, 974 (1970).
- ¹¹See, for example, G. K. L. Wong and Y. R. Shen, *Phys. Rev. Lett.* **30**, 895 (1973); also R. L. Carman, R. Y. Chiao, and P. L. Kelley, *ibid.* **17**, 1281 (1966); N. Bloembergen and P. Lallemand, *ibid.* **16**, 81 (1966).
- ¹²See, for example, Y. R. Shen, *Prog. Quantum Electron.* **4**, 1 (1975); *Rev. Mod. Phys.* **48**, 1 (1976), and the numerous references therein.
- ¹³See, for example, I. Haller, H. A. Huggins, and J. Freiser, *Mol. Cryst.* **16**, 53 (1972) and Ref. 1.